pure metal powders. The ignition of graphite (carbon) will probably depend on the presence of other fuel components. Aluminum may be hypergolic with ClF_3 under some conditions.

Reference

[1] Rhein, R. A., "Ignition of Metals With ClF_3 and ClF_5 for use as Spacecraft Chemical Heaters," *Journal of Spacecraft and Rockets*, Vol. 6, No. 11, Nov. 1969, pp. 1328–1329.

Phase Change Solidification Dynamics

ANTHONY O. UKANWA,* FRANKLIN J. STERMOLE,† AND JOHN O. GOLDEN‡
Colorado School of Mines, Golden, Colo.

Nomenclature

C_p = specific heat
h = total height of n-hexadecane in test cell
h_a = dimensionless spatial increment = Δz
H_f = heat of fusion, cal/g or Btu/lb
K = thermal conductivity
k_a = dimensionless time increment = $\Delta\tau_o = \Delta\tau$
N = total number of spatial nodes
p = k_a/h_a^2
R = number of completely solidified space nodes
S = dimensionless height of solid phase formed
T, T_a = temperature and ambient temperature, respectively
T_e = equilibrium temperature of solidification
t = time, sec or min
t^* = time interval from start of cooling to the start of solidification at the bottom plate
x_j = fraction of partly-solidified node that is solid, by the jth time step
Y = height of solid phase formed, cm or in.
y = spatial coordinate
z = dimensionless spatial coordinate
α = thermal diffusivity
λ = dimensionless constant = α_S/α_L
ρ = density, g/cm³ or lb/ft³
τ_0, τ = dimensionless times, presolidification and solidification
τ_0^* = dimensionless time corresponding to t^*
θ = dimensionless temperature

Subscripts

i,j = finite spatial and time increments, respectively
Lo = presolidification problem (liquid)
L,S = liquid and solid phases

Introduction

CANDIDATE phase-change materials for thermal control systems for spacecraft should have equilibrium melting temperatures that are close to the acceptable range for the design media for electronic equipment, 40°F–150°F, with heats of fusion $\geq$100 Btu/lbm, and they should be noncorrosive, nontoxic, chemically inert and stable, with low vapor pressures, small volume changes, and negligible subcooling. Normal (long-chain) paraffins with even numbers of carbon atoms are most widely considered.

Carslaw and Jaeger[1] pointed out the basic nonlinear nature of phase-change problems. A survey of phase-change problems and the experimental study of different test cells are presented in Ref. 2. Bannister[3] emphasized the need to study nucleation theory as a basis for the study of subcooling phenomena in solidification problems. An approximate one-dimensional mathematical model, neglecting the effects of convection was presented by Pujado, Stermole, and Golden.[4] Ehrlich[5] gave the implicit finite-difference equations for the one-dimensional melting problem with a variable heat flux or heat input specified as a function of time. Grozka[6] included the effects of gravity, magnetic and electric fields, and convective currents; she pointed out that the pure-conduction problem with phase change is valid so long as the liquid phase remains stable, and that natural convection must be considered after the Rayleigh number reaches 1720 for a layer of fluid either heated from below or cooled from above. Many other papers are reviewed in a survey by Muehlbauer and Sunderland.[7] This Note is based on Ref. 8, in which implicit finite-difference equations were obtained for the one-dimensional model of the solidification of n-hexadecane and were put into tridiagonal matrix forms and solved by Gauss elimination and back substitution.

Theoretical Analysis

The problem to be studied is the solidification of n-hexadecane in a cell of height h (between plates) and constant cross-sectional area in the plane perpendicular to the axis, y of the cell (Fig. 1). The temperature profile and the rate of solidification are to be determined using a one-dimensional model along the y axis and assuming that unsteady state conditions obtain. The effects of convection are assumed to be negligible, because mixing that occurs when solidification takes place is minimized by having the cell cooled from the bottom, so that the solid formed at the bottom of the cell remains there, and ρ_S and ρ_L are nearly equal for n-hexadecane between 262°K and 310°K, so that the net velocity of the interface between the solid and the liquid phases is near zero. It is further assumed that the cell and its content are at ambient temperature T_a initially,

$$T_{Lo}(y,0) = T_a \text{ at } t = 0 \text{ for } 0 \leq y \leq h \quad (1)$$

and the temperatures of the inside faces of the bottom and the top plates of the cell are functions, $f_1(t)$ and $f_2(t)$, of time, respectively:

$$T_{Lo}(0,t) = f_1(t) \text{ at } y = 0 \quad (2)$$

$$T_{Lo}(h,t) = f_2(t) \text{ at } y = h \quad (3)$$

With these definitions, knowledge of the temperature profiles of the inside faces of the two plates, say by polynomial fits of

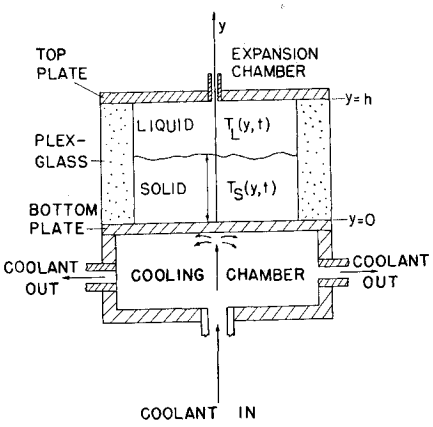

Fig. 1 Axial section of test cell.

Received October 14, 1970; revision received November 23, 1970. This work was done as a part of NASA research contract NAS8-30511, Space Sciences Laboratory, Marshall Space Flight Center, Huntsville, Ala.

* Graduate Research Assistant and Doctoral Candidate, Department of Chemical and Petroleum Refining Engineering.
† Professor, Department of Chemical and Petroleum Refining Engineering.
‡ Associate Professor, Department of Chemical and Petroleum Refining Engineering.

experimentally determined temperatures of these faces, makes it unnecessary to write energy balances on the plates in order to solve the problem for n-hexadecane.

The heat transfer problems are divided into two parts: a "presolidification" problem, covering heat transfer in liquid n-hexadecane from the time ($t = 0$), when cooling of the bottom plate is initiated, to the time t^* when the equilibrium temperature of solidification T_e is reached at the bottom plate; and a "solidification" problem, covering heat transfer in solid and liquid and the rate of solidification from the time t^* to a later time when the entire content of the cell is frozen. In the presolidification problem, the governing equation is

$$\alpha_L[\partial^2 T_{Lo}(y,t)]/\partial y^2 = [\partial T_{Lo}(y,t)]/\partial t,\ 0 \le t \le t^* \qquad 0 \le y \le h \tag{4}$$

The initial and boundary conditions are given by Eqs. (1–3). Note that $T_{Lo}(0,t^*) = f_1(t^*) = T_e$. By means of the following dimensionless variables, $\theta = T(y,t)/T_e$, $z = y/h$, $\tau_o = t\alpha_L/h^2$, and $\tau_o^* = t^*\alpha_L/h^2$, Eq. (4) and the boundary conditions become

$$\frac{\partial^2\theta_{Lo}(z,\tau_o)}{\partial z^2} = \frac{\partial\theta_{Lo}(z,\tau_o)}{\partial\tau_o},\ 0 \le z \le 1,\ 0 \le \tau_o \le \tau_o^* \tag{5}$$

$$\theta_{Lo}(0,\tau_o) = f_1(\tau_o)/T_e \text{ at } z = 0 \tag{6}$$

$$\theta_{Lo}(1,\tau_o) = f_2(\tau_o)/T_e \text{ at } z = 1 \tag{7}$$

$$\theta_{Lo}(z,0) = T_a/T_e \text{ at } \tau_o = 0,\ 0 \le z \le 1 \tag{8}$$

By means of Taylor series expansions, the following implicit finite-difference equations are obtained from Eq. (5) and its boundary conditions:

$$\theta_{Lo_0,j+1} = f_{1j+1}/T_e \tag{9}$$

$$\theta_{Lo_N,j+1} = f_{2j+1}/T_e \tag{10}$$

$$-\frac{p}{2}\theta_{Lo_{i-1},j+1} + (1+p)\theta_{Lo_i,j+1} - \frac{p}{2}\theta_{Lo_{i+1},j+1} = \frac{p}{2}\theta_{Lo_{i-1},j} + (1-p)\theta_{Lo_i,j} + \frac{p}{2}\theta_{Lo_{i+1},j} \tag{11}$$

$$1 \le i \le N-1$$

Eqs. (9–11) are used to calculate temperature profiles until $\theta_{Lo} > 1.0$ at some j^*, but ≤ 1.0 at $j^* + 1$. At such a time, the time τ_o^* (corresponding to t^*) is calculated from the equation $\tau_o^* = k_a(j^* + r)$ where $r = (\theta_{Lo_0,j^*} - 1.0)/(\theta_{Lo_0,j^*} - \theta_{Lo_0,j^*+1})$. The temperature profile at τ_o^* is calculated from the equation

$$\theta_{Lo_i,j^*+1} = rp\theta_{Lo_{i-1},j^*} + (1-2rp)\theta_{Lo_i,j^*} + rp\theta_{Lo_{i+1},j^*} \tag{12}$$

for $1 \le i \le N$, where $\theta_{Lo_0,j^*+1} = 1.0$. The presolidification temperature is taken to be completely known and so is the time interval t^*.

In the solidification problem: both solid and liquid are present, and the heat transfer problem becomes

$$\frac{\alpha_S\partial^2 T_S(y,t)}{\partial y^2} = \frac{\partial T_S(y,t)}{\partial t},\ t > t^*,\ 0 \le y \le Y(t) \tag{13}$$

$$\alpha_L\frac{\partial^2 T_L(y,t)}{\partial y^2} = \frac{\partial T_L(y,t)}{\partial t},\ t > t^*,\ Y(t) \le y \le h \tag{14}$$

Using the additional dimensionless variables, $S = Y/h$, $\tau = (t - t^*)\alpha_L/h^2 = \tau_o - \tau_o^*$, Eqs. (13) and (14) are transformed to

$$\lambda\partial^2\theta_S/\partial z = \partial\theta_S/\partial\tau,\ \tau > 0,\ 0 < z < S \tag{15}$$

$$\partial^2\theta_L/\partial z^2 = \partial\theta_L/\partial\tau,\ \tau > 0,\ S < z < 1 \tag{16}$$

subject to the following conditions:

$$\theta_S(S,\tau) = \theta_L(S,\tau) = 1.0 \text{ at } z = S \text{ for } \tau \ge 0 \tag{17}$$

$$M(\partial\theta_S/\partial z) - J\partial\theta_L/\partial z = dS/d\tau \text{ at } z = S \text{ for } \tau \ge 0 \tag{18}$$

$$\theta_L(z,0) = \theta_{Lo}(z,\tau_o^*) \text{ at } \tau = 0 \text{ (at } \tau_o = \tau_o^*) \tag{19}$$

$$S(0) = 0,\ \tau = 0 \tag{20}$$

$$\theta_S(0,0) = f_1(\tau = 0)/T_e = 1.0,\ \tau = 0,\ z = 0 \tag{21}$$

$$\theta_L(1,0) = f_2(\tau = 0)/Te = \theta_{Lo}(1,0),\ \tau = 0 \tag{22}$$

where $\lambda = \alpha_S/\alpha_L$, $M = \lambda C_{pS}Te/H_f$ and $J = (\rho_L/\rho_S)C_{pL} \times Te/H_f$. Conditions (17, 18, and 20) describe the interface.

Any of the following situations may occur at the two-phase interface: the freezing point crosses A) no space grid line B) one, C) two, or D) three or more grid lines. Each case requires special equations for the points near the interface. The following equations are obtained by Taylor-series expansion: for the solid phase,

Case A: $R(j+1) - R(j) = 0$;

$$-\frac{2\lambda p x_{j+1}}{1+x_{j+1}}\theta_{S_{R-1},j+1} + (2\lambda p + x_{j+1})\theta_{S_R,j+1} = x_{j+1}\theta_{S_R,j} + \frac{2\lambda p}{1+x_{j+1}} \tag{23}$$

$$-\frac{\lambda p}{2}\theta_{S_{i-1},j+1} + (1+\lambda p)\theta_{S_i,j+1} = \frac{\lambda p}{2}\theta_{S_{i-1},j} + (1-\lambda p)\theta_{S_i,j} + \frac{\lambda p}{2}\theta_{S_{i+1},j},\ 1 \le i \le R-1 \tag{24}$$

Case B: $R(j+1) - R(j) = 1$; and the governing equations are Eq. (24) and

$$-\frac{2\lambda p x_{j+1}}{1+x_{j+1}}\theta_{S_{R-1},j+1} + \left(2\lambda p + \frac{x_{j+1}}{a_R}\right)\theta_{S_R,j+1} = \frac{x_{j+1}}{a_R} + \frac{2\lambda p}{1+x_{j+1}} \tag{25}$$

where $a_R = x_{j+1}/(1 - x_j + x_{j+1})$, and

$$-\lambda p\theta_{S_{i-2},j+1} + (1+2\lambda p)\theta_{S_{i-1},j+1} - \lambda p\theta_{S_i,j+1} = \theta_{S_{R-1},j},\ R-1 \le i \le R \tag{26}$$

Case C: $R(j+1) - R(j) = 2$; and the proper equations are Eqs. (24) and (25) and

$$-\lambda p a_{R-1}\theta_{S_{R-2},j+1} + (2\lambda p a_{R-1} + 1)\theta_{S_{R-1},j+1} - \lambda p a_{R-1}\theta_{S_R,j+1} = 1 \tag{27}$$

where $a_{R-1} = (1 + x_{j+1})/(2 - x_j + x_{j+1})$ and a_R is now $x_{j+1}/(2 - x_j + x_{j+1})$.

Case D: $R(j+1) - R(j) \ge 3$; we halve the time step, make a new estimate of $R_{(j+1)}$ and check whether $R(j+1) - R(j)$ has a value that satisfies one of Cases A to C. If one of these cases applies, we use the appropriate group of equations. If none has yet occurred, we again halve the time step and continue this process until one of Cases A to C has occurred. After calculating temperatures with the appropriate equations, we return to the regular time increment for the next time step. For the liquid phase, no matter the value of $R_{(j+1)} - R_{(j)}$, the following groupings hold: $0 \le R(j+1) \le N-3$, then

$$(2 - x_{j+1})(1 + 2p - x_{j+1})\theta_{LR+1,j+1} - 2p(1 - x_{j+1})\theta_{LR+2,j+1} = (2 - x_{j+1})(1 - x_{j+1})\theta_{LR+1,j} + 2p \tag{28}$$

$$-\frac{p}{2}\theta_{L_{i-1},j+1} + (1+p)\theta_{L_i,j+1} - \frac{p}{2}\theta_{L_{i+1},j+1} = \frac{p}{2}\theta_{L_{i-1},j} + (1-p)\theta_{L_i,j} + \frac{p}{2}\theta_{L_{i+1},j} \tag{29}$$

$$R+2 \le i \le N-1$$

$$\theta_{LN,j+1} = (f_2)_{j+1}/T_e \tag{30}$$

To calculate S_{j+1}, the height of solid which has formed by the $(j + 1)st$ time step, we use the following equations: for

$$\begin{gathered} 0 \leq x_{j+1} \leq 1, \text{ and } 0 \leq R \leq N \\ S_{j+1} = h_a[R(j + 1) + x_{j+1}] \end{gathered} \tag{31}$$

If

$$\tfrac{1}{4} < x_{j+1} \leq \tfrac{3}{4}$$

then

$$S_{j+1} = S_j + h_a p(M\sigma_S - J\sigma_L), 1 \leq R \leq N - 2 \tag{32}$$

If $0 \leq x_{j+1} \leq \frac{1}{4}$, we use Eq. (32) for $2 \leq R \leq N - 3$ with σ_S replaced by σ'_S. If $\frac{3}{4} < x_{j+1} \leq 1$, we use Eq. (32) for $2 \leq R \leq N - 3$ with σ_L replaced by σ_L':

$$\sigma_S = \frac{x_{j+1}}{1 + x_{j+1}} \theta_{S_{R-1},j+1} - \frac{1 + x_{j+1}}{x_{j+1}} \theta_{S_R,j+1} + \frac{1 + 2x_{j+1}}{x_{j+1}(1 + x_{j+1})} \tag{33}$$

$$\sigma_L = \frac{2 - x_{j+1}}{1 + x_{j+1}} \theta_{L_{R+1},j+1} - \frac{1 - x_{j+1}}{2 - x_{j+1}} \theta_{L_{R+2},j+1} - \frac{3 - 2x_{j+1}}{(1 - x_{j+1})(2 - x_{j+1})} \tag{34}$$

$$2\sigma'_S = (1 + 2x_{j+1})\theta_{S_{R-2},j+1} - 4(1 + x_{j+1})\theta_{S_{R-1},j+1} + (3 + 2x_{j+1})\theta_{S_R,j+1} \tag{35}$$

$$2\sigma'_L = (2x_{j+1} - 5)\theta_{L_{R+1},j+1} + (8 - 4x_{j+1})\theta_{L_{R+2},j+1} + (2x_{j+1} - 3)\theta_{L_{R+3},j+1} \tag{36}$$

Note that the equations for calculating temperature profiles are in tridiagonal matrix forms which are easily solved by Gauss elimination and back substitution. First, a reasonable value is assumed for S_{j+1}, say $S_{j+1} = h_a/2$, and R and x_{j+1} are calculated from Eq. (31). These are then used in the equations for the temperature profiles, and the temperatures are in turn used to calculate a new value of S_{j+1}. The two values of S_{j+1} are compared, and if they are within a certain allowable limit (found from truncation errors and stability criteria) of each other, S_{j+1} is taken to be known and a new time step is made using $S_{j+1} = S_j + \Delta S_j$ where $\Delta S_j = S_j - S_{j-1}$, and the procedure is repeated. If two consecutive values of S_{j+1} for the same time step have not converged, the iterative method is used until they do. The stability criteria require that $0 < p \leq p_{\max}$ where $p_{\max} = \min(1/\lambda, \frac{1}{2})$. This implies that $0 < k_a \leq k_{a_{\max}}$ where $k_{a_{\max}} = h_a{}^2\min(1/\lambda, \frac{1}{2})$.

Equipment and Results

The external dimensions of the test cell (Fig. 1) were 5 in. × 5 in. × 3.5 in. high. The auxiliary elements were a thermocouple assembly, one 4-channel-continuous-temperature recorder, a pump, and a refrigerator that circulated methanol as the coolant. The cell was composed of a cooling chamber sealed with solder to one face of an $\frac{1}{8}$-in.-thick copper plate (the bottom plate); a plexiglas frame 1.5-in. high, which formed the chamber for the n-hexadecane; and another $\frac{1}{8}$-in.-thick copper plate (the top plate) that sealed the plexiglas frame. Both plates carried thermocouples fixed to their inside faces. The temperatures of the plates were fitted [$f_1(t)$ and $f_2(t)$] by exponentials of the form $A + Be^{-c(t)t}$, where A and B are constants depending on the initial and the final steady-state temperatures of the plates, and $c(t)$ is a polynomial in t of degree 5 or fewer (Table 1).

Table 1 Least-squares fit, $f_1(t)$ and $f_2(t)$, to experimentally measured temperatures of the bottom and top plates, respectively; T_a = 297.8°K

Final steady-state temperature of bottom plate = 262.7°K

$f_1(t) = 262.7 + 35.1e^{-c_1 t} \pm 0.4$°K

$f_2(t) = 262.7 + 35.1e^{-c_2 t} \pm 0.1$°K

$c_1 = 6.5019191 \times 10^{-2} + 0.40147416t - 0.14185947t^2 + 2.2468639 \times 10^{-2}t^3 - 1.6686646 \times 10^{-3}t^4 + 4.7213390 \times 10^{-5}t^5$

$c_2 = -3.3434403 \times 10^{-4} + 2.4737272 \times 10^{-4}t - 5.7413214 \times 10^{-6}t^2 + 5.2857290 \times 10^{-8}t^3 - 1.7660905 \times 10^{-10}t^4$

t is measured in minutes: $0 \leq t \leq 61$

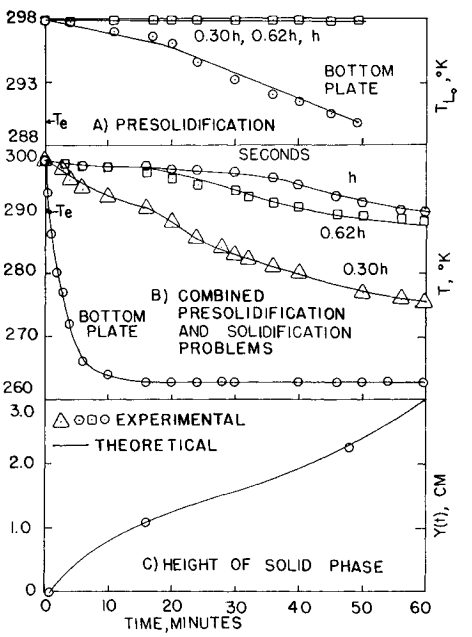

Fig. 2 Results for a typical run.

Figure 2 shows that the experimental and theoretical results for a typical run agree closely for the presolidification problem (Fig. 2A), but in the solidification problem, the theoretical result indicates a faster rate of cooling than indicated experimentally, particularly as the freezing front approaches the top plate. One of the many possible explanations of this deviation is that the one-dimensional analysis does not account for heat gains from the surroundings in the other directions. This heat would slow down the rate of solidification and would become more significant as the solidification approached the top plate. In addition to extraneous heat gains the effects of convection which were neglected and all the approximations made in setting up the model tend to increase the deviation of the model from the true situation.

Conclusions

The numerical analysis developed in this Note has proved to be a good unidimensional model for the solidification of *n*-hexadecane. However, the consideration of partially-solidified elements may be eliminated when considering two- or three-dimensional models. Instead of assuming constant but different properties for each phase, one may use temperature-dependent properties to get more accurate results. Better-controlled and better-measured heat transfer techniques will certainly improve the results.

References

[1] Carslaw, H. S. and Jaeger, J. C., *Conduction of Heat in Solids*, 2nd ed., Oxford Univ. Press, Oxford, England, 1959, pp. 282–296.

[2] Bentilla, E. W., Sterrett, K. F., and Karre, L. E., "Thermal Control by Use of Fusible Materials," Final Rept., NSL65-16-1, Contract NAS8-11163, 1966, Northrop Corp., Hawthorne, Calif.

[3] Bannister, T. C., "Space Thermal Control Using Phase Change," TMX-53402, 1966, NASA.

[4] Pujado, P. R., Stermole, F. J., and Golden, J. O., "Melting of a Finite Paraffin Slab as Applied to Phase-Change Thermal Control," *Journal of Spacecraft and Rockets*, Vol. 6, No. 3, March 1969, pp. 280–284.

[5] Ehrlich, L. W., "A Numerical Method of Solving a Heat Flow Problem with Moving Boundary," *Journal of Association for Computing Machinery*, Vol. 5, No. 2, 1958, pp. 161–176.

[6] Grozka, P. G. and Fan, C., "Thermal Control by Freezing and Melting," Interim Rept., HREC-1123-1, LMSC/HRECA 791342, Contract NAS8-21123, 1968, Lockheed Missiles & Space Co., Huntsville, Ala.

[7] Muehlbauer, J. C. and Sunderland, J. E., "Heat Conduction with Freezing and Melting," *Applied Mechanics Review*, Vol. 18, No. 12, 1965, pp. 951–959.

[8] Ukanwa, A. O., *Phase Change Solidification Phenomena*, M.S. thesis, T-1289, Feb. 1970, Colorado School of Mines Golden, Colo.

Flow Coefficients for Supersonic Nozzles with Comparatively Small Radius of Curvature Throats

L. H. Back* and R. F. Cuffel†
Jet Propulsion Laboratory, Pasadena, Calif.

Nomenclature

a	=	sound speed
A	=	cross-sectional area
C_D	=	mass flow coefficient, $\dot{m}/\dot{m}_{1-D}$
$C_{D\text{inv}}$	=	two-dimensional inviscid flow coefficient
D	=	diameter
$f(\gamma)$	=	$\{\gamma[2/(\gamma+1)]^{(\gamma+1)/(\gamma-1)}\}^{1/2}$
$\dot{m}$	=	mass flow rate
$\dot{m}_{1-D}$	=	one-dimensional value, $f(\gamma)p_t A_{th}/(RT_t)^{1/2}$
M	=	Mach number
p	=	pressure
r, r_{th}	=	radius and throat radius, respectively
r_c	=	throat radius of curvature
R	=	gas constant
$Re_{D_{th}}$	=	throat Reynolds number, $(\dot{m}D/A\mu^*)_{th}$
T	=	temperature
u	=	velocity
γ	=	specific heat ratio
δ^*	=	displacement thickness
λ, σ	=	divergent and convergent half-angles
μ, ρ	=	viscosity and density, respectively

Subscripts and superscripts

a	=	ambient back pressure
e	=	edge of boundary layer
i,t	=	inlet and stagnation conditions
th,w	=	throat and wall conditions
$(\ )^*$	=	sonic condition

Introduction

THIS Note is concerned with the determination of the mass flow rate through choked nozzles with emphasis on comparatively small radius of curvature throats. In the flow regime investigated (throat Reynolds numbers larger than 10^6) viscous (boundary layer) effects are not believed to be significant,[1] so that the flow field can be regarded as essentially isentropic. Mass flux nonuniformities for the air flows studies are then primarily caused by the throat configuration (Fig. 1)[2] and result in reduced mass flow rates below the ideal one-dimensional flow value, since in either the subsonic flow region near the centerline or the supersonic region near the wall the mass flux is less than at the sonic condition. The nozzles considered have circular-arc throats with values of the ratio of throat radius of curvature to throat radius r_c/r_{th} extending from 2 down to nearly 0, corresponding to a sharp-edged throat. Measured values of the flow coefficient C_D are presented for nozzles recently tested at the Jet Propulsion Laboratory (JPL) and for nozzles which have been previously tested in other investigations (Table 1). Of interest is the relative correspondence of the earlier measurements by Durham[3] that span a large range of r_c/r_{th} to the recent data since there is some question about their absolute magnitude because of the accuracy of the measurements that were made in a blow down facility. These measurements taken collectively provide a basis on which to evaluate the effect of r_c/r_{th} on the flow coefficient and to appraise existing and recently developed prediction methods for isentropic flow by other investigators.

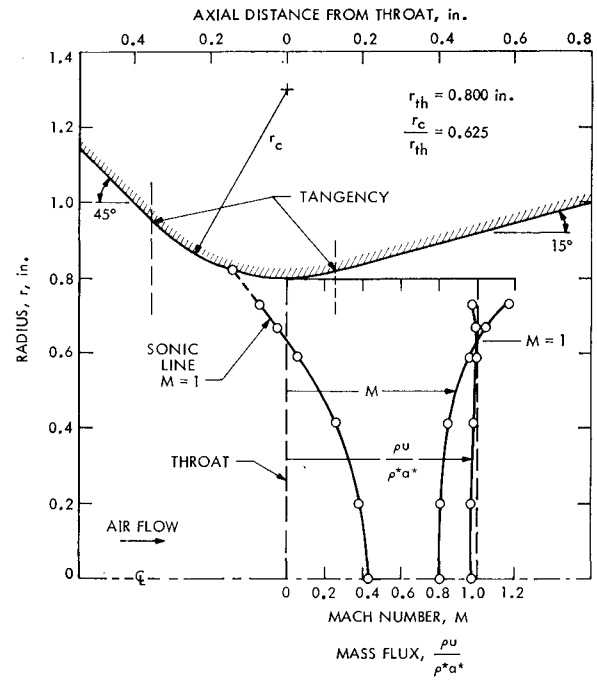

Fig. 1 Flow in the throat region of an axisymmetric nozzle. The Mach number and mass flux profiles are at the throat plane; the measurements are from Ref. 2 with air flow p_t = 70 psia, T_t = 540°R, $Re_{D_{th}}$ = 2.8 × 10^6, adiabatic wall.

Present Tests

Tests were conducted in the auxiliary flow channel of the JPL hypersonic wind tunnel.[4] Air flowed steadily through a venturi meter, a plenum chamber, a contraction section, a constant-diameter duct, and the nozzle, into an evacuated chamber. Stagnation pressure measured with a pitot tube ranged from 25 to 100 psia. Stagnation temperature, measured with a thermocouple upstream of the nozzle inlet where the flow speed was low, was ~530°R. The nozzles tested had relatively steep convergent sections with convergent half-angles (σ) of 75° and 90° and with r_c/r_{th} = 0.25 and 0.49, respectively. Nozzles with these shapes are being considered for rocket engine applications because they are shorter

Received October 23, 1970; revision received December 3, 1970. This work presents the results of one phase of research carried out at the Jet Propulsion Laboratory, California Institute of Technology, under Contract NAS 7-100, sponsored by NASA.

* Member Technical Staff, Propulsion Research and Advanced Concepts Section. Associate Fellow AIAA.

† Senior Engineer, Propulsion Research and Advanced Concepts Section. Member AIAA.